

Advanced modelling of deposit formation in biomass furnaces – investigation of mechanisms and comparison with deposit measurements in a small-scale pellet boiler

Dr.-Ing. Kai Schulze¹, Dipl.-Ing. Dr. Robert Scharler^{1,2,3}, DI Markus Telian⁴,
Prof. Dipl.-Ing. Dr. Ingwald Obernberger^{1,2,3}

¹Bioenergy 2020+ GmbH, Inffeldgasse 21b, A-8010 Graz, Austria
Tel.: +43/316/8739223; Fax: +43/316/8739202; E-mail: kai.schulze@bioenergy2020.eu

²BIOS BIOENERGIESYSTEME GmbH, Inffeldgasse 21b, A-8010 Graz, Austria

³Institute for Process and Particle Engineering, Graz University of Technology, Austria

⁴Hovalwerk AG, FL-9490 Vaduz (Liechtenstein)

ABSTRACT

A CFD model for deposit formation has been developed at the Austrian Bioenergy competence centre Bioenergy 2020+ in cooperation with the Graz University of Technology. At the present state, the model considers the condensation of ash vapours, deposition of coarse salt-rich and silica-rich fly ash particles, brittle and ductile erosion of the deposit layer by non-sticky particles, aerosol formation and deposition under consideration of a single particle size class as well as the influence of the growing deposit layer on heat transfer (heat conduction, radiative emissivity of the surfaces) in the furnace and the boiler.

In order to verify the model, test runs with a 70 kW pellet furnace (Hovalwerk AG) were performed. The modelling results were validated against accompanying deposit formation measurements (mass and chemical composition) in different locations of the plant. The comparison of simulations with experiments showed, that the locations of strong deposit build-up could be reproduced. Moreover, the application of the advanced model shows the influence of the mechanisms on deposit formation at different locations in the plant. The interaction between condensation, aerosol formation and the deposition of coarse fly ash particles is illustrated.

Keywords: *biomass combustion, ash deposition, CFD simulation*

1. INTRODUCTION AND OBJECTIVES

Due to the rising energy consumption worldwide combustion of alternative fuels such as agricultural fuels and different waste fractions becomes increasingly important for the production of heat and power. But these fuels also increase the risk of ash related problems like slagging in furnaces as well as fouling and corrosion in boilers. Furthermore, fine particulate emissions play an important role because ecological concerns. Boiler manufacturers and operators thus have to find strategies to take into account these problems in order to be competitive.

In order to predict and finally to control the formation of ash deposits as well as particulate emissions occurring in biomass combustion units, much R&D work has already been performed over the last years. ([3], [15], [16]). Models for ash release and deposit formation have been developed in order to investigate the complex

interactions of the deposit formation processes and to influence them concerning reduced probabilities of ash deposit and fine particulate formation in biomass fired boilers. Computational Fluid Dynamics (CFD) is a promising way to evaluate the complex interactions between the governing mechanisms of deposit formation, allowing for a spatially and temporally resolved simulation of the turbulent reactive flow as well as the heat and mass transfer on the walls. CFD simulations for the design and optimisation of furnaces and boilers have already been successfully performed by several authors ([1] [2] [9]) but in most cases the models are limited to only certain fractions of ash forming compounds or to single mechanisms.

Modelling of ash deposit formation using CFD is still a challenge due to its high complexity and uncertainties of the underlying models (e.g. turbulence models in regions of transition from laminar to turbulent flow regimes). Furthermore, the CFD-calculations are very time consuming. Limitations of the computational power restrict the model regarding its complexity.

Nevertheless, aware of these limitations, CFD models can be used to get qualitative information about the deposit formation process in order to provide information about influences regarding different boundary conditions.

Within this frame, a very detailed CFD model for ash deposit formation in biomass fired boilers has been developed as efficient process analysis and design tool. It considers the condensation of ash vapours, the deposition of coarse salt-rich and silica-rich fly ash particles, brittle and ductile erosion of the deposit layer by non-sticky particles, aerosol formation and deposition under consideration of a single particle size class as well as the influence of the growing deposit layer on heat transfer (heat conduction and radiative emissivity of the surfaces) in the boiler.

In order to evaluate the reliability and accuracy of the model, test runs for a 70 kW pellet furnace (HOVALWERK AG) were performed. The numerical data were compared with measurements of deposited mass and chemical composition of the deposits for different plant zones.

Furthermore, a sensitivity study was carried out to investigate the influence of the different deposit formation mechanisms on the entire deposit build-up and their interactions.

2. MODEL SETUP

Overview

The deposit formation model is implemented in the CFD Code FLUENT 12 using user defined functions (UDF). **Fig. 1** illustrates an overview about the sub-models implemented in the overall CFD model for ash deposit formation.

The calculation of solid biomass combustion on the grate and the release of flue gas components from the fuel bed is performed using an empirical biomass fuel model based on experimental data [14] in order to provide the boundary conditions for the subsequent simulation of the turbulent reactive flow. The calculation of the gas phase combustion is based on the Realizable k- ϵ model for turbulence, the Discrete Ordinate Model for radiation and the Eddy Dissipation model in combination with a global methane 3-step reaction mechanism including the flue gas components CH₄, CO, CO₂, H₂, H₂O and O₂ for gas phase combustion. A detailed description of the CFD model for biomass grate furnaces can be found in Scharler [14].

The deposit build-up is determined within a post-processing step based on the flow and gas phase combustion simulation. The empirical fixed bed release model was extended in order to determine the release of ash vapours and the entrainment of coarse fly ash particles from the grate to provide the boundary conditions for the calculation of the transport of the ash vapours as well as the trajectories of the coarse fly ash particles. Subsequently, ash vapour condensation on the boiler walls, aerosol formation and deposition on the boiler walls are calculated. The calculation of deposition of coarse fly ash particles on boiler walls is based on two different stickiness approaches - a viscosity approach for silica-rich particles and a melting approach for salt-rich particles.

The condensation of the ash vapours as well as the deposition of coarse fly ash particles and aerosols contribute to the time-dependent build-up of the deposit layer. The growth of the deposit layer influences the heat transfer due to changes of the thermal resistance and emissivity of the layer as a function of its chemical composition, temperature, structure and thickness. Furthermore, erosion of deposits by coarse fly ash particles is considered.

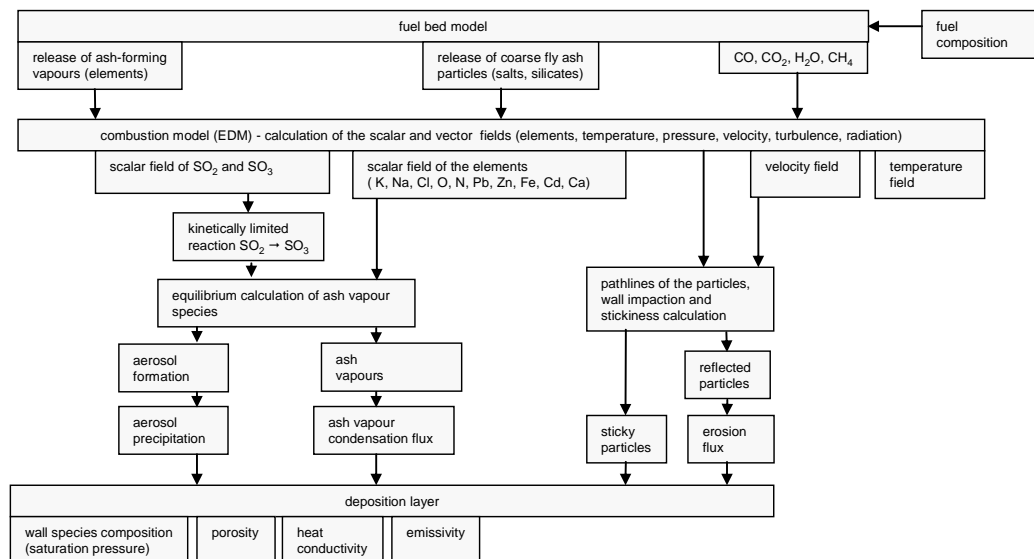


Fig. 1: Flow chart of the CFD-based deposit formation model for biomass-fired boilers

In the following, a short description of the most relevant sub-models for ash deposit formation is given:

Wall condensation and fine particle formation

During solid fuel combustion, ash forming vapours are released from the fuel bed into the gas phase. The mass flux and the composition of the ash components depend on the temperature in the fuel bed as well as the composition of the fuel. Due to the cooling of the flue gas or the contact with cooled walls, the vapour pressure of the components decreases. If the vapour pressure becomes lower than the saturation pressure of the ash vapour, the aggregate state changes to liquid or solid phases. Consequently, fine particles are formed in the gas phase, which form deposits on walls or are emitted. Furthermore, when the vapour pressure on the wall is lower than in the boundary layer, condensation occurs.

Ash forming vapours are involved in a complex reaction system. Here, with exception of the kinetically limited formation of sulphates, it is assumed that reactions between ash forming vapours are fast in comparison to local residence time of the flue

gas. In this case, the chemical composition can be determined by thermodynamic equilibrium calculations.

In case of the formation of sulphates, a kinetic approach was applied. According to Christensen [12] the formation of SO₃ from precursors (SO₂) is limited rather than the final formation of sulphates. In this model, the global reaction rate according to (Christensen) based on an Arrhenius approach, was implemented in combination with the Eddy Dissipation Model. Furthermore, in order to reduce the mathematical effort to model the transport of the ash vapours, the deposit formation model considers the transport of the elements (C, S, Cl, K, Na) instead of all the species as these elements are the most relevant ones regarding aerosol formation in wood pellet boilers [17]. To calculate condensation fluxes to the walls or fine particle formation, ash vapour pressures of species are determined by thermodynamic equilibrium calculations in combination with the In-Situ Adaptive Tabulation Algorithm (ISAT) [6] for the reduction of calculation times.

The condensation of ash vapours is modelled based on a mass transfer approach using the analogy of mass transfer to the convective heat transfer to determine the mass transfer coefficient β ([7]). Here, \dot{N}_{cond} represents the condensation flux per area, α the heat transfer coefficient, c_p the heat capacity and ρ the density of the flue gas.

$$\dot{N}_{cond} = \frac{\alpha}{c_p \cdot \rho} Le^{m-1} \cdot (c_\infty - c_w) \quad (0.1)$$

Here, the Lewis number Le as well as the exponent m were set to unity.

While for c_∞ thermodynamic equilibrium calculations are carried out only under consideration of gaseous components, for the wall concentration c_w also liquid and solid phases at the surfaces have to be considered. In this work, the components KCl, (KCl)₂, K₂SO₄, K₂CO₃, NaCl, (NaCl)₂ and Na₂SO₄ are considered as ash forming vapours.

Similarly to condensation, the calculation procedure is implemented to calculate the super-saturation of ash components in the flue gas to describe the nucleation of the ash vapour components as initial aerosol formation process. The nucleation rate is calculated according to Friedlander [11], which is based on the classical theory of nucleation:

$$I_{nucl} = 2 \cdot \frac{p_i}{\sqrt{2 \cdot \pi \cdot m_m \cdot k_B \cdot T}} \cdot V_m^{2/3} \cdot n_m \cdot \sqrt{\frac{\sigma \cdot V_m^{2/3}}{k_B \cdot T}} \cdot \exp\left(-\frac{16 \cdot \pi \cdot \sigma^3 \cdot V_m^2}{3 \cdot (k_B \cdot T)^3 \cdot \ln(S)^2}\right) \quad (0.2)$$

Here, p_i is the vapour pressure of the nucleating compound i , m_m is the mass of a molecule calculated from the molar weight and Avogadro's number, V_m is the volume of a molecule calculated from the liquid density and Avogadro's number, n_m is the molecule concentration in the gas, σ is the surface tension of the nucleating compound, S is the saturation ratio ($=p_i/p_{sat}$ with p_{sat} = saturation pressure of the nucleating compound).

Besides the formation of new particles by nucleation, the model also considers condensation of ash vapours on the surface of existing aerosol particles. For this purpose, the condensation flux is determined by

$$\begin{aligned}
 I_{kond} &= \frac{F_i \cdot MW_i \cdot 6}{\rho_i \cdot d_p^3 \cdot \pi} \\
 F_i &= \frac{2 \cdot \pi \cdot D_i \cdot d_p \cdot (p_i - p_{i,sat}^*)}{k_B \cdot T}
 \end{aligned}
 \tag{0.3}$$

with ρ_i as density of the condensing compound, D_i as diffusion coefficient of the condensing compound in the gas phase and MW_i as molecular weight of the condensing compound.

At the present state of development, a constant particle size (10^{-7} m) was assumed. Consequently, nucleation and condensation results in a change of the number of fine particles formed.

The deposition of fine particles is considered by Fick's law for diffusion and thermophoresis according to:

$$v_{th} = \frac{\nu_{gas} \cdot K_{th}}{T_p} \nabla T_{gas}
 \tag{0.4}$$

K_{th} is the so-called thermophoretic coefficient, which is determined by Talbot [10] ν_{gas} the viscosity of the gas, T_p the temperature of the particle and ∇T_{gas} the local temperature gradient prevailing in the gas phase. Deposition mechanisms of fine particles due to inertial impaction, gravitational settling as well as diffusio-phoresis are neglected up to now, but it is known, that they also play a minor role [18].

Deposition of coarse fly ash particles

The transport of coarse fly ash is modelled using an Lagrangian approach, which is already implemented in the CFD code FLUENT (Discrete Phase Model). Once a particle impacts the wall, either its kinetic energy is high enough to rebound from the surface, or the particle sticks to the wall. The total sticking probability p_{tot} of the particle depends on the properties (sticking probabilities p) of the wall and the particle (Walsh):

$$p_{tot} = p_{wall} \cdot p_{part} + p_{wall} \cdot (1 - p_{part}) + (1 - p_{wall}) \cdot p_{part}
 \tag{0.5}$$

In this model, a viscosity approach for silica rich particles is used to calculate the sticking probability as a ratio of the reference viscosity μ_{ref} and the viscosity of the particle at a certain temperature μ_{part} . Here, the reference viscosity is calculated as a function of the kinetic energy of the particle ([13])

$$\begin{aligned}
 p_{part,silicates} &= \frac{\mu_{ref}}{\mu_{part}} & \mu_{part} > \mu_{ref} , \\
 p_{part,silicates} &= 1 & \mu_{part} \leq \mu_{ref} .
 \end{aligned}
 \tag{0.6}$$

The melt approach according to Backman [4] was applied for salt-rich particles and deposit layers. If the liquid fraction of the particle or the deposit layer is below 15 %, a sticking probability $p_{part, salts}$ of 0 is assumed. Above this fraction, a linear correlation of the stickiness from 0 to 100% is assumed up to a melt fraction of 0.7. The amount of the melt fraction is calculated by thermodynamic equilibrium calculations considering condensed phases (salt mixtures, slags).

Since a particle and a deposit layer consist of a mixture of salt and silica rich material, the melt approach as well as the viscosity approach have to be combined. Similarly to

an approach of Kaehr [1], the sticking probabilities of both approaches are combined using the mass weighted average:

$$P_{part} = \frac{m_{silicate}}{m_{salt} + m_{silicate}} \cdot P_{part,silicates} + \frac{m_{salt}}{m_{salt} + m_{silicate}} \cdot P_{part,salt} \quad (0.7)$$

Particle erosion

If the coarse fly ash particles do not stick on the walls, they rebound. Depending on the particle velocity and the impact angle, this process causes erosion of the deposit layer. In literature, two main mechanisms are distinguished: brittle erosion and ductile erosion. When particles impact on a surface, the loss of kinetic energy during the impact is absorbed by the deposit surface through plastic deformation and commonly by the formation of cracks. This so-called brittle erosion has its maximum at a wall-normal impact angle. In contradiction, at low impact angles ductile erosion becomes relevant, which can be described as the cutting of material from the layer. The weighting of both sub-mechanisms depends on the material properties of the particle and the wall material, the impact angle as well as the kinetic energy of the particle.

In order to consider these erosion effects by coarse fly ash particles, the model from Neilson and Gilchrist based on the system of equations (0.8) has been implemented and the erosion rate is computed as the superposition of the ductile (\dot{W}_d) and brittle (\dot{W}_b) erosion mechanisms.

$$\dot{W} = \dot{W}_d + \dot{W}_b \quad [kg / s]$$

$$\dot{W} = \underbrace{\frac{\frac{1}{2} \dot{M} V^2 \cos^2 \alpha \sin n \alpha}{\phi}}_{\dot{W}_d (A)} + \underbrace{\frac{\frac{1}{2} \dot{M} (V \sin \alpha - K)^2}{\epsilon}}_{\dot{W}_b (B)} \quad [\alpha < \alpha_o] \quad (0.8)$$

$$\dot{W} = \underbrace{\frac{\frac{1}{2} \dot{M} V^2 \cos^2 \alpha}{\phi}}_{\dot{W}_d (C)} + \underbrace{\frac{\frac{1}{2} \dot{M} (V \sin \alpha - K)^2}{\epsilon}}_{\dot{W}_b (B)} \quad [\alpha > \alpha_o]$$

\dot{W}	erosion flux	[kg/s]
V	particle velocity	[m/s]
\dot{M}	particle mass flux	[kg/s]
α	particle collision angle (see fig. 2.10)	[°]
K	threshold velocity	[m/s]
α_o	transition impingement angle	[°]
ϕ	Ductile Wear Factor	[Nm/kg]
ϵ	Brittle Wear Factor	[Nm/kg]

In this equation, part (A) and (C) account for cutting wear, while part (B) represents the erosion by brittle wear.

3. TEST RUN RESULTS

PLANT DESCRIPTION AND OPERATING CONDITIONS

In order to evaluate the CFD-based deposit formation model described in chapter 2, test runs with a 70 kW wood pellet furnace including fuel analyses, boiler heat load, air mass fluxes, conventional flue gas and dust measurements (concentrations and

particle size distributions for the definition of boundary conditions for the CFD simulations) has been performed. Furthermore, grate ash, fly ash and hard ash deposit measurements in different plant zones (mass and chemical composition) have been investigated. Fig. 2 provides an overview about the main parts of the pellet furnace

The furnace is divided into a primary combustion zone (PCZ) located in the rear part of the burner tube, which is cooled by the secondary air (see Fig. 2) and a water cooled secondary combustion zone (SCZ). After the combustion of the fuel in the burner tube (PCZ), the released flue gas is mixed with secondary air supplied by nozzles at the exit of the burner tube. At the top of the SCZ, the heat exchanger tube bundle is installed. The automatic cleaning system for the heat exchanger tubes was not installed for the purpose of the model check.

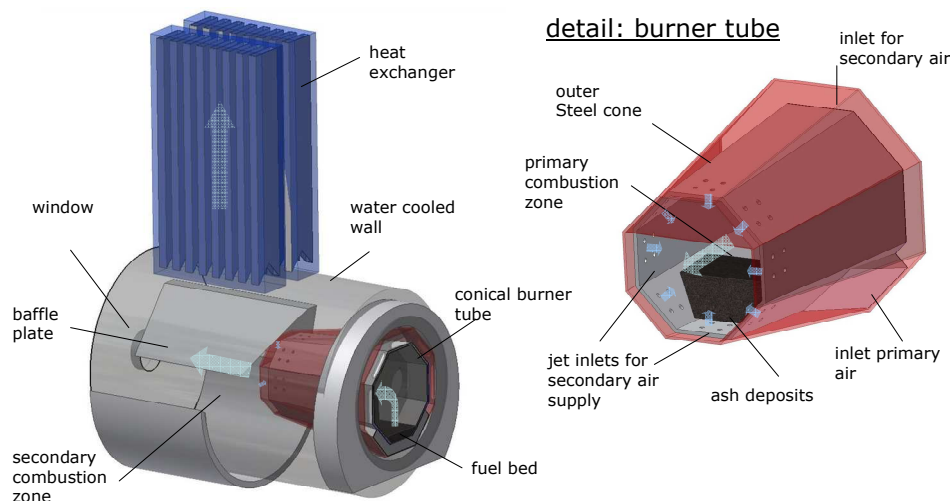


Fig. 2: Overview about the Biolyt 70 boiler

The most relevant operating conditions of the pellet furnace during the test runs and the chemical composition of the ash are shown in Table 1.

Table 1: Operating conditions of the furnace for the combustion simulation (left) and concentration of ash forming elements in the wood pellets (right)

parameter	value	unit	element	unit	wood pellets
fuel	wood pellet		Si	mg/kg d.b.	199.00
fuel flow rate	15.67	kg/h	Ca	mg/kg d.b.	1,000.00
ash content	0.40	wt.% d.b.	Mg	mg/kg d.b.	118.00
moisture content	6.80	wt.% d.b.	K	mg/kg d.b.	402.00
boiler load	74	kW _{th}	Na	mg/kg d.b.	38.20
primary air mass flux	31	kg/h	S	mg/kg d.b.	64.70
secondary air mass flux	122	kg/h	Cl	mg/kg d.b.	44.00
total air ratio	1.79	-	Zn	mg/kg d.b.	9.88
primary air ratio	0.36	-	Pb	mg/kg d.b.	5
adiabatic flame temperature	1,329	°C	Fe	mg/kg d.b.	26.30
cooling water temperature	62	°C	Mn	mg/kg d.b.	168.00
			Al	mg/kg d.b.	34.20
			P	mg/kg d.b.	49.50
			Ti	mg/kg d.b.	1.89

TEST RUN RESULTS

Fig. 3 shows the bottom ash as well as the ash deposits found after an operation time of 69 h of nominal load in the SCZ. The mass fractions of the ash deposited at

different locations of the walls of the furnace and at the heat exchanger have been investigated to validate the CFD-based deposit formation model.

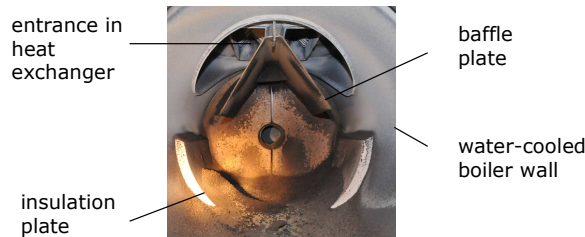


Fig. 3: Deposits and bottom ash formed during the combustion of wood pellet in a 70 kW pellet boiler (HOVALWERK AG), view from the outlet of the burner tube

Most of the ash was found as bottom ash on the insulation plate on the bottom of the SCZ as well as inside the burner tube. **Fig. 4** shows the total masses (a) and the distribution of the different ash fractions in different plant sections.

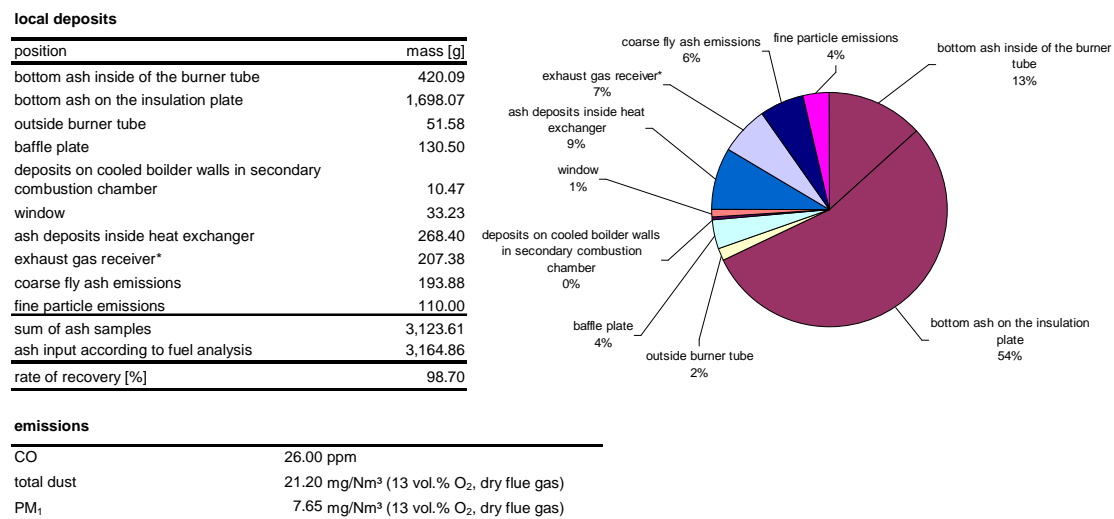


Fig. 4: Mass of ash deposits found in different plant zones and emissions over an operation time of 69 h of full load

According to the measurements 6 % of the entire ash is entrained as coarse fly ash and 4 % is released as fine particle emissions ($< 1\mu\text{m}$). Other 9 % are condensates and coarse fly ash particles deposited on the walls of the heat exchanger. The overall mass balance regarding ashes found in comparison to the ash input with the fuel closes well which underlines the plausibility of the measurements performed. The burnout conditions were very good as indicated by the low CO emissions. The chemical composition of the ashes is presented in **Fig. 5**. The bottom ash the ash in the burner tube as well as the coarse fly ash particles deposited on the window and exhaust gas channel consist of Si, Ca, Mg, K, Mg and small amounts of P. This composition is representative for silica rich materials. On the other hand, the chemical composition of fine particles, determined by low pressure impactor measurements, shows semi- and easily volatile elements: K, Na, S, Cl and Zn. The composition of the other fractions represents mixtures of coarse fly ash particles and condensed species.

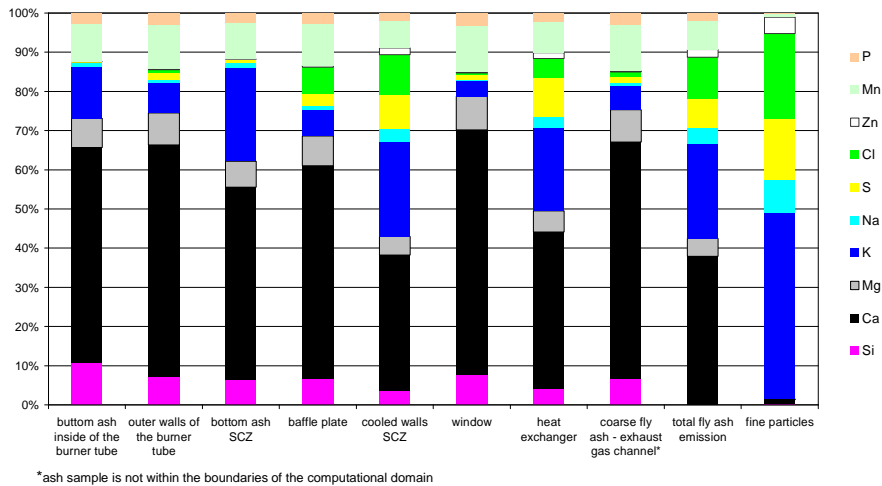


Fig. 5: Chemical composition of the different ash fractions (given in wt.%)

Since the release behaviour of the ash vapours and the entrainment of coarse fly ash particles into the gas phase strongly depends on the chemical composition of the fuel and the local conditions in the fuel bed (like temperature, oxygen content and primary air flow trough the fuel bed) for which currently no reliable model exists, the release of ash forming vapours and coarse fly ash particles was determined from the test run. The released mass of the aerosol forming elements K, Na, Cl and S from the fuel bed was calculated from the difference of the mass of these elements found in the bottom ash fractions and in the coarse fly ash fractions (under the assumption that the coarse fly ash has the same composition than the bottom ash when entrained from the fuel bed) and the amount of these elements supplied with the fuel. The amount of coarse fly ash entrained from the fuel bed was calculated by subtracting the amount of bottom ash formed and the amount of ash vapours released from the total mass of ash supplied with the fuel. Since the deposits from the exhaust gas channel (see Fig. 5) mainly consist of coarse fly ash particles, their chemical composition was used to calculate the particle stickiness properties of the model.

Fig. 6 gives an overview about the concentrations of the ash forming elements released to the gas phase determined by mass balances. Furthermore, the chemical composition of the coarse fly ash particles entrained from the fuel bed is presented.

element	wt.% of element input with the fuel	element	wt.% dry ash
K	25	Si	3.35%
Na	58	Ca	25.20%
S	87	Mg	3.39%
Cl	96	K	12.30%
		Na	0.65%
		S	0.34%
		Cl	0.07%
		Zn	0.04%
		Pb	0.00%
		Fe	0.65%
		Mn	4.78%
		Al	0.54%
		P	1.26%
		Ti	0.04%

Fig. 6: Percentage of aerosol forming elements released from the fuel (left) and chemical composition of the coarse fly ash particles (right)

Due to the small amounts of Zn released from the fuel bed, its influence on condensation/fine particle formation was neglected within this simulation.

NUMERICAL RESULTS

In a first step, CFD simulations with each sub-model (deposition by coarse fly ash particles, fine particle formation) have been performed separately, in order to investigate the influence of the different sub-mechanisms on the deposit formation process.

In a second step, simulation runs have been performed considering all sub-models implemented within the deposit formation model. Ash deposit rates in different plant zones as well as the emissions of coarse fly ash and fine particles are compared with measurements to check and evaluate the simulations.

AERSOL FORMATION

Fig. 7 illustrates results of the fine particle sub-model (direct wall condensation as well as aerosol formation and deposition are considered).

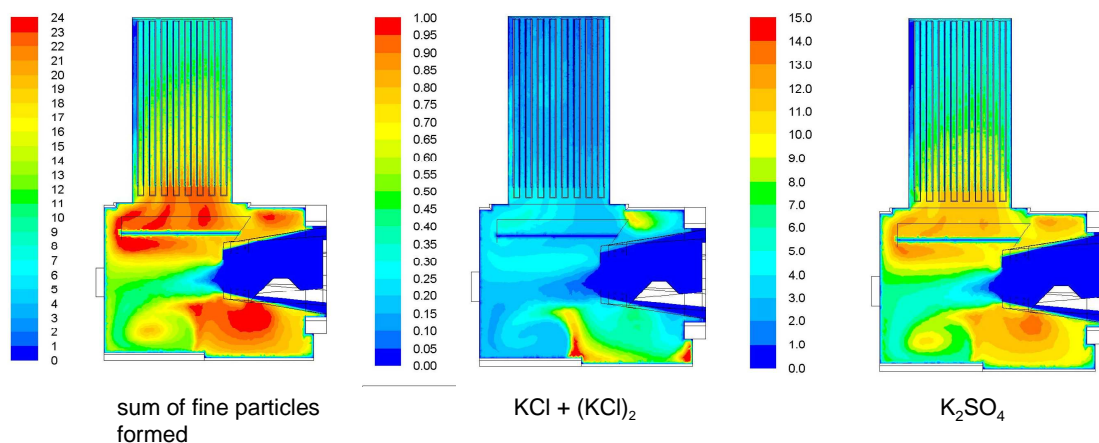


Fig. 7: Simulation results regarding aerosol formation: a) total particle concentrations [mg/Nm^3], b) fine particles formed by nucleation/condensation of KCl [mg/Nm^3] c) fine particle mass formed by nucleation/condensation of K_2SO_4 [mg/Nm^3]

While on the left hand side the total fine particle emissions are shown, the other pictures show the contribution of KCl and the dimer $(\text{KCl})_2$ (middle) as well as K_2SO_4 (right). Different fine particle formation behaviour can be observed in the burner tube and in the SCZ due to different flue gas temperatures in these regions. Since the temperatures inside of the burner (see **Fig. 8 b**) are above $1,000^\circ\text{C}$, the first formation of fine particles can only be observed at the outlet of the burner. In the cooled SCZ, chlorides and sulphates are formed.

The results of the fine particle model can, at present, only be regarded as qualitative information. The distribution between sulphates and chlorides formed are qualitatively not correct (if compared with the analysis results of the aerosols sampled at boiler outlet – see **Fig. 9**). The concentration of sulphates is over predicted at present which makes a check and evaluation of the sulphation kinetics implemented in the model necessary.

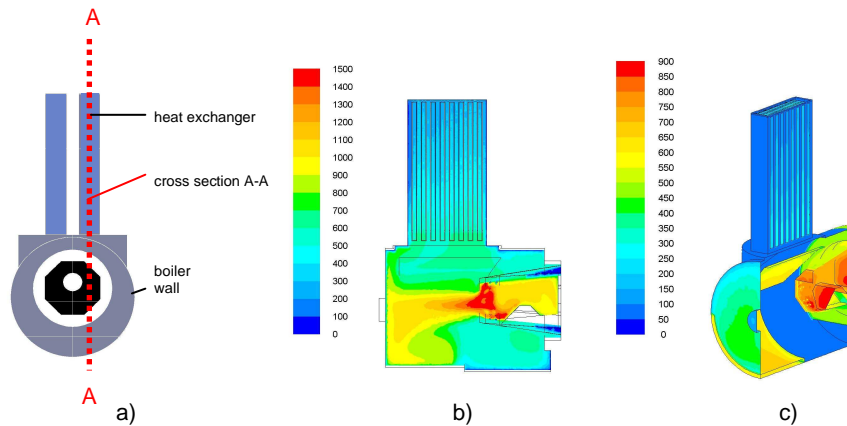


Fig. 8: Calculated flue gas temperatures ($^{\circ}\text{C}$) in the vertical cross section A-A of the boiler b) as well as wall temperature of the biomass boiler c)

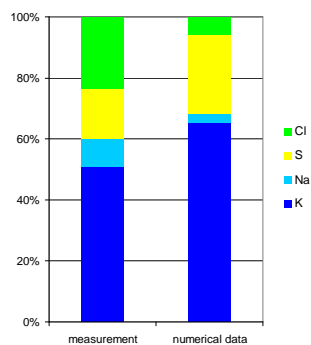


Fig. 9: Comparison of experimental and numerical data regarding the chemical composition of fine particles (given in wt.% d.b.)

Further numerical optimisations regarding the convergence behaviour are necessary to achieve a higher accuracy of the fine-particle sub-model.

DEPOSITION OF COARSE FLY ASH PARTICLES

Fig. 10 a) shows deposition mass fluxes caused by the impaction of coarse fly ash particles (other deposition processes are not considered). The main part of the particles is captured by the inner hot walls of the burner tube (see **Fig. 8 a**).

Also in the SCZ, the model predicts a high sticking probability of the particles impacting on the insulation plate. Since the mass fraction of silica-rich components of the particles amounts to 98%, the stickiness of the particles is almost entirely determined by the viscosity approach. **Fig. 10 b)** presents the stickiness of the particles of different diameters calculated for an impact velocity of 5 m/s using equation (0.6). Due to the high flue gas temperature at the outlet of the burner tube (maximum of 1500°C as indicated in **Fig. 8 b**), the particles reach a temperature of approximately 900°C at an impact. As a result of the model, the main part of the particles contributes to deposit formation.

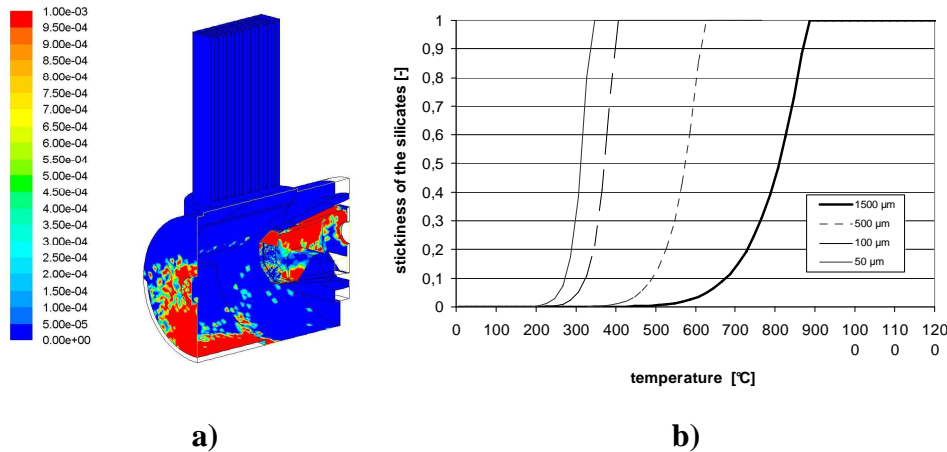


Fig. 10: a) Deposit mass flux caused by coarse fly ash particles (kg/m²h); b) stickiness of the silicate fraction of the coarse fly ash particles calculated by equation (0.6) using a particle impact velocity of 5 m/s

OVERALL DEPOSIT BUILD-UP

In **Fig. 11** a) the experimental data from test runs are compared with a combined simulation considering condensation of ash vapours, aerosol formation and deposition as well as deposition of coarse fly ash particles (overall model).

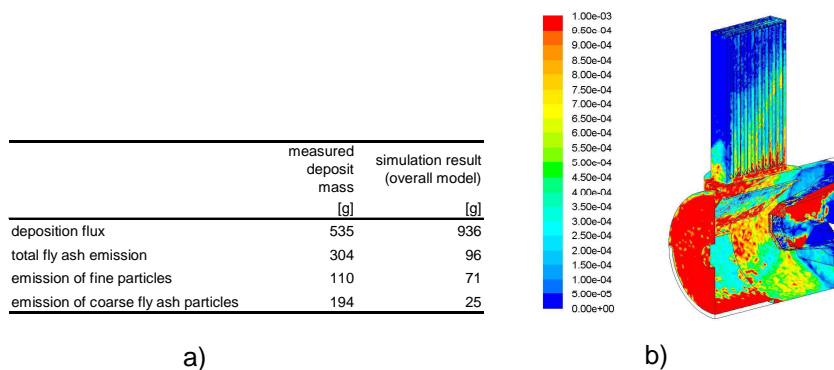


Fig. 11: Comparison of experimental and numerical data (from the overall model) regarding deposition and emission results a) and local deposition rates (kg/m²h) b)

The comparison with experimental data shows that the measured deposition flux is lower than the simulation result almost by a factor of two, while the predicted fine particle emissions are in a rather good agreement with the measurements. As already discussed, the reasons can mainly be found in the overestimation of the stickiness of the coarse fly ash particles. As a consequence, the influence of the erosion model can be neglected within this simulation because the high stickiness results in no relevant particle rebound rates after their impact on the walls.

4. SUMMARY AND CONCLUSIONS

The application of the deposit formation model illustrates the influence of the different mechanisms on deposit formation in the plant. The interaction between condensation, aerosol formation and the deposition of coarse fly ash particles is shown.

The comparison of model predictions with emissions of coarse fly ash particles shows, that the stickiness of the silica-rich particles is over predicted by the model. Further experimental investigations concerning the modelling of the viscosity of biomass ashes as described in [19] as well as the reference viscosity of the stickiness approach regarding silica-rich particles (e.g. described in [13]) are necessary to increase the accuracy of the stickiness approach used.

The results of the aerosol formation model in combination with the condensation model are qualitatively in a rather good agreement with experimental findings, since gas to particle formation of alkali sulphates and chlorides occurred in the right temperature ranges. Quantitatively, the amount of alkali sulphates formed is too large which demands for a check of the sulphation kinetics implemented. In addition, some deviations from the measurement results must be expected, since the model contains some simplifications (e.g. constant material properties) as well as no modelling of the particle size distribution.

Moreover, further improvements to achieve more stable solutions and to reduce the computational time are necessary (currently at least one month of calculation time is necessary for the fine particle simulation). Additionally, in order to improve the prediction accuracy of the CFD based aerosol formation model, the particle size distribution shall be considered in the future. Furthermore, physical and chemical properties of the fine particles will be implemented in detail.

Concluding, it can be stated that an advanced tool for an efficient design of biomass furnaces and boilers is under development. The influence of the fuel fired and operation conditions on the deposit formation processes can be investigated in detail considering the relevant mechanisms already in the design phase of the plant and thus allowing for appropriate measures in order to reduce ash deposit formation and to take proper choices regarding material selection in terms of corrosion issues. The model can already deliver qualitatively correct results, some adjustments regarding the stickiness behaviour of coarse fly ash particles and the sulphation kinetics shall also make it applicable for quantitative evaluations in the near future. As further development steps, model enhancements concerning the convergence behaviour of the model, the consideration of aerosol particle size distributions as well as the deposit build-up in heat exchanger tube-bundles are foreseen.

5. REFERENCES

- [1] S. K. Kaer, L. Rosendahl, Extending the modelling capacity of CFD Codes applied to biomass-fired boilers, Proc. ECOS; Copenhagen, Denmark. Jun 30-Jul 2 (2003) 251–264.
- [2] D. Bouris, G. Bergeles, Particle-Surface Interactions in heat-exchanger fouling, Transactions of the ASME 118 (1996) 574-581
- [3] H. Kaufmann, T. Nussbaumer, L. Baxter et al., Deposit formation on a single cylinder during combustion of herbaceous biomass, Fuel 79 (2000) 141-151

- [4] R. Backman, M. Hupa, B-J. Skrifvars, Predicting superheater deposit formation in boilers burning biomass, Proceedings of the conference on impact of mineral impurities in solid fuel combustion (1997) 405-416.
- [5] P. M. Walsh, A. N. Sayre, D. O. Loehden et al., Deposition of bituminous coal ash on an isolated heat exchanger tube: effects of coal properties on deposit growth, Progress in Energy Combustion Science 16 (1990) 327-346.
- [6] S. B. Pope, ISAT-CK (Version 3.0) User's Guide and Reference Manual, Ithaca Combustion Enterprise, LLC, Ithaca, USA (2000)
- [7] H. D. Baehr, K. Stephan, Wärme- und Stoffübertragung, 2nd edition, Springer, Berlin. 1996
- [8] M. Forstner, G. Hofmeister, M. Jöller et al., CFD simulation of ash deposit formation in fixed bed biomass furnaces and boilers, Progress in Computational Fluid Dynamics, Vol. 6, Nos. 4/5 (2006) 248-261.
- [9] P. Venturini, D. Borello, C. Iossa et al., Modeling of multiphase combustion and deposit formation in a biomass-fed furnace, Energy 35 (2010) 3008-3021
- [10] L. Talbot, R. K. Cheng, R. W. Schefer et al., Thermophoresis of particles in a heated boundary layer, Journal of Fluid Mechanics, 101 (1980) 737-758.
- [11] S. K. Friedlander, Smoke, dust and haze; John Wiley & Sons, New York 1977 ISBN 0-471-01468-0.
- [12] Christensen, K.A., Stenholm, M. and Livberg, H., 1998: The formation of submicron aerosol particles, HCl and SO₂ in straw fired boilers, Journal of Aerosol Science, 29, 421-444
- [13] K. Schulze, G. Hofmeister, M. Joeller et al., Development and evaluation of a flexible model for CFD simulation of ash deposit formation in biomass fired boilers. In: Proc of the Int. Conf. "Impacts of Fuel Quality on Power Production", EPRI report No. 1014551 (2007), pp.7-95 to 7-113, EPRI (Ed.), Palo Alto, CA; USA
- [14] R. Scharler, Entwicklung und Optimierung von Biomasse-Rostfeuerungen durch CFD-Analyse, Ph.D. thesis, Graz University of Technology, Graz, Austria 2001
- [15] F. C.C. Lee, F. C. Lockwood, Modelling ash deposition in pulverised coal-fired applications, Progress in Energy and Combustion Science, 25 (1999) 117-132.
- [16] C. Mueller, B. J. Skrifvars, R. Backman et al., Ash deposition prediction in biomass fired fluidized bed boilers – combination of CFD and advanced fuel analysis, Progress in Computational Fluid Dynamics, 3 (2003) 112-120.
- [17] T. Brunner, G. Bärnthaler, I. Obernberber, Evaluation of parameters determining PM emissions and their chemical composition in modern residential biomass heating appliances. In: Proc. of the int. Conf. World BIOENERGY 2008, May 2008, Jönköping, Sweden, ISBN 978-91-977624-0-3, pp.81-86, Swedish Bioenergy Association (Ed.), Stockholm, Sweden 2008
- [18] T. Brunner, Aerosols and coarse fly ashes in fixed-bed biomass combustion, in: book series "Thermal Biomass Utilization", Volume 7, ISBN 3-9501980-4-0, published from BIOS BIOENERGIESYSTEME GmbH, Graz, Austria 2006
- [19] S. Arvelakis, F. J. Frandsen, Rheology of fly ashes from coal and biomass co-combustion, Fuel 89 (2008) 3132-3140

6. ACKNOWLEDGEMENTS

The work presented was supported by the Kplus program of the BIOENERGY2020+ GmbH. The financial support of the Austrian Research Promotion Agency as well as of the state governments of Lower Austria and Styria and of the City of Graz as well as of the companies BIOS BIOENERGIESYSTEME GmbH, MAXXTEC AG, Hovalwerk AG, KWB Kraft und Wärme aus Biomasse GesmbH is gratefully acknowledged. The deposit measurements were performed in cooperation with Hovalwerk AG, Liechtenstein.